Available online at www.sciencedirect.com

ScienceDirect

Physics Procedia 77 (2015) 34 – 41

Physics Procedia

International Conference on Laser Applications at Accelerators, LA3NET 2015

X-ray Photoemission Spectroscopy Studies of Cesium Antimonide Photocathodes for Photoinjector Applications

Irene Martini[ab]*, Eric Chevallay[a], Valentin Fedosseev[a], Christoph Hessler[a], Holger Neupert[a], Valentin Nistor[a], Mauro Taborelli[a]

[a]*CERN, CH-1211, Geneva 23, Switzerland*
[b]*Politecnico di Milano, Piazza L. Da Vinci 32, 20133 Milano, Italy*

Abstract

Within the CLIC (Compact Linear Collider) project, feasibility studies of a photoinjector option for the drive beam as an alternative to its baseline design using a thermionic electron gun (Geschonke et al. [1]) are on-going. This R&D program covers both the laser and the photocathode side. Cesium antimonide cathodes were produced at CERN by co-deposition onto copper substrates and characterized by photoemission and by XPS (X-ray Photoemission Spectroscopy) analysis. A systematic study on newly produced and used photocathodes was conducted in order to correlate the surface composition to the photoemissive properties.

Peer-review under responsibility of the University of Liverpool

Keywords: Photocathode, Photoinjector, XPS, Surface Characterization, Cesium Antimonide

1. Introduction

The high-charge PHIN RF photoinjector is currently used for feasibility study of the CLIC drive beam photoinjector option although the current PHIN gun is not specially designed for such purpose. The electron source requirements for the CLIC drive beam are very demanding. The main challenge for a drive beam photoinjector is to achieve 8.4 nC bunch charge, 140 μs train length and 500 MHz bunch repetition rate together with reasonable cathode lifetime.

A detailed investigation of the performance of Cs_2Te photocathodes used in combination with UV laser beam was conducted by Hessler et al. [2] in the PHIN RF photoinjector to study the lifetime dependence on the beam parameters and on the vacuum level. Cs_2Te photocathodes showed an improved 1/e lifetime from 38 to 250 hours (for 2.3 nC and

* *E-mail address:* irene.martini@cern.ch

Peer-review under responsibility of the University of Liverpool
doi:10.1016/j.phpro.2015.11.007

350 ns train length) after the vacuum system upgrade and allowed the production of 9.2 nC bunch charge (large size laser beam, 50 ns train length).

Fulfilling all the CLIC requirements at the same time is still a challenge. In particular the laser pulse energy in UV for such long pulse trains is currently limited due to a degradation of the beam quality during the 4th harmonics conversion process. Using green laser beam in combination with Cs_3Sb cathodes could overcome this limitation.

Over the past years excellent quantum efficiency (QE) values were obtained for Cs_2Te cathodes produced by co- deposition at CERN (Chevallay [3]), therefore the same procedure was used to deposit Cs_3Sb onto the OFE (Oxygen Free Electronic) copper substrates (Martini et al.[4]). The cathodes are produced in a dedicated laboratory which is equipped with a deposition chamber and a 70 kV DC gun beam line.

Detailed studies of Cs_3Sb cathode fundamental properties, such as life-time and dark current, were performed in the PHIN RF photoinjector (Hessler et al. [5], Hessler et al. [6]).

In order to investigate the correlation between the photoemissive properties and the cathodes surface composition, a UHV transfer vessel compatible with the CERN XPS (X-Ray Photoemission Spectroscopy) setup was commissioned and two Cs_3Sb cathodes (#199, #200) were studied. Following the tests in the PHIN RF photoinjector, it was possible to give an explanation to the deeply degraded photoemissive properties of cathode #199 in terms of the surface composition thanks to the XPS analysis. The surface of cathode #202 as grown was probed to investigate the quality of the deposition process, which is characterized by a variability in the maximum QE values reached from one cathode to another. Cathode #202 was then used in the DC gun setup for high average current (120 μA) lifetime measurement. Although the beam parameters and the environmental conditions are quite different with respect to the RF photoinjector operation, the QE degradation over time has a similar trend (Hessler et al. [6]). XPS analyses were performed on the same cathode surface to study the changes in composition from newly produced to after use cathode.

2. Experimental procedure

Both Cs_3Sb and Cs_2Te are produced by a thin film deposition technique called co-deposition (Chevallay [3], Martini et al. [4]). CERN-made Sb and Te evaporators, fabricated on molybdenum crucibles, and commercial Cs dispensers (SAES Getters) are used as sources. The different chemical elements (Cs, Te or Sb) are evaporated at the same time to mix together in the vapour phase before the deposition onto the OFE copper substrate. The substrate is heated at 120° C for Cs_3Sb deposition and kept at room temperature for Cs_2Te. The deposition chamber is equipped with two thickness monitors which can measured the deposition rate of the two evaporated elements separately thanks to two shielding masks. The co-deposition process is optimized in order to reach a maximum in the QE, whose evolution is monitored in real time during deposition by illuminating the cathode with a pulsed green laser beam at λ=532 nm (or UV laser beam at λ =266 nm for Cs_2Te) and collecting the photoemitted electrons with a circular anode. As a result the total evaporated quantity of Cs and Sb (or Te) vary between tens to hundreds of nanometers among different photocathodes.

The preparation chamber is attached to a beam line equipped with a 70 kV DC electron gun. The cathode surface is scanned with a small spot size laser beam while the produced charge is measured with a WCM (Wall Current Monitor) downstream of the DC gun in order to get the QE maps at different stages of the cathode life: right after the deposition and after having been used for beam production (see Fig. 1). The laser used for QE maps and during the cathode production is a Nd:YAG (Spectron SL802) operated at 10 Hz and 5 ns pulse duration.

For lifetime measurements in the DC gun setup, instead the second harmonic (λ=532 nm) of a high repetition rate Nd:YAG (Quantronix 532 DP-1) laser system operated at 2 kHz repetition rate and 100 ns pulse duration was used.

One cathode per time can be transferred from the production laboratory to the XPS analysis setup under UHV condition (background pressure: $P=10^{-11}$ mbar) to preserve the highly chemical reactive surfaces. XPS spectra were collected by a commercial system (SPECS GmbH) equipped with a hemispherical energy analyser (Phoibos 150) and a monochromatized Al x-ray source. The energy scale is calibrated with the position of the Cu $2p_{3/2}$ and Au $4f_{7/2}$ lines. The average pressure in the XPS analysis chamber is $P\sim5x10^{-10}$ mbar.

3. Results and discussion

A detailed XPS analysis allow to identify and quantify the relative elemental composition of the surface as well as to distinguish the chemical bonding states of such elements. A correlation between the chemical composition of the surface and the QE was found. The poor photoemissive properties are accompanied by surface contamination and deviation from the optimal stoichiometry of the cathodes composition.

3.1. Measurements on cathode #202 (Cs_3Sb) as newly produced

Fig. 2 (a) shows the XPS wide range spectrum taken on the surface of cathode #202 as grown together with the relative elemental composition of the detected elements. The measured ratio Cs/Sb is 0.6, much lower than the optimal stoichiometry. As explained by Spicer [7] Cs_3Sb is a p- type semiconductor in which acceptor levels are due to a slight excess of antimony. Nonetheless the calculated stoichiometric ratio of cathode #202 indicates a much stronger deficiency of cesium which is explained by the presence of a Sb-rich phase on the cathode surface, as shown in the peaks model proposed in Fig. 2 (b). There are in fact many stable Cs-Sb compounds (Sangster et al. [8]) that are likely to be produced during the deposition process (Sommer [9]). A further argument to such explanation is that the maximum measured value of the QE at 532 nm is only 3.5% (see Fig. 1 (a)), less than half compared to the best Cs_3Sb cathode produced at CERN with the same preparation setup and procedure (QE=7.5%, Martini et al. [4]) and much lower than QE=20% obtained in photomultiplier applications (Sommer [9]).

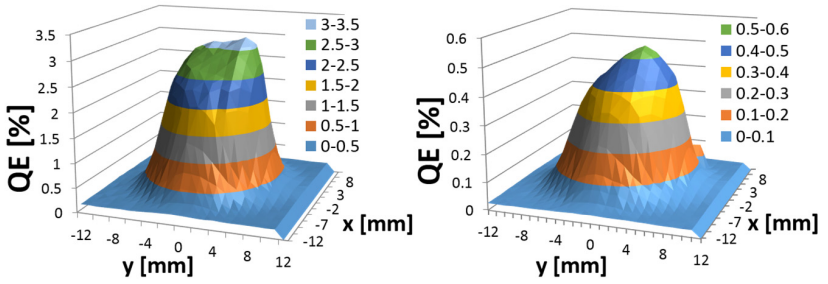

Fig.1. QE maps of cathode #202 (Cs_3Sb) (a) as newly produced; (b) after lifetime measurements in the DC gun setup.

The XPS measurement taken with high resolution in the energy region of the antimony 3d core levels, which exhibit the typical doublet pair structure due to the spin orbit splitting, shows the overlapping 1s core level of oxygen (Fig. 2 (b)). The fit of the experimental data shown in Fig. 2 (b) is obtained by using Gaussian-Lorentzian peaks with fixed area ratio (1.5) between the two components of the doublet pair (Sb $3d_{5/2}$ and Sb $3d_{3/2}$) and cross-checking the resulting spin–orbit shift between each corresponding peak (about 9.3 eV). This allowed the identification of the oxygen contribution as the residual intensity. The following discussion will refer only to the most intense peak of any doublet pairs for simplicity.

Two chemical states of antimony were identified: Sb^{3-} (as in the compound Cs_3Sb, peak at 526 eV) and a peak at 527.3 eV which is attributed to an alkali deficient Cs-Sb compound (labelled as Sb^{x-}, where x refers to the oxidation state which for this compound is unknown). The attribution of the peak at 526 eV is in agreement with Soriano et al. [10]. A similar peak as the Sb-rich phase one is reported by Bates et al. [11] at 527 eV. Two oxygen peaks were identified under the broad shoulder: the peak at 531.7 eV, which was attributed to cesium sub-oxide (Cs_3O_{11}) already identified by Bates et al. [11] and Soriano et al. [10], and a peak at 533.9 eV. Electrons from O1 s orbital of such high binding energy are normally related to adsorbed molecular water (Spitzer et al. [13], Linn et al. [14]).

In baked UHV systems as the ones in which the cathode was introduced the partial pressure of water is very low, nonetheless some molecules of water can react with the alkali antimonide surfaces.

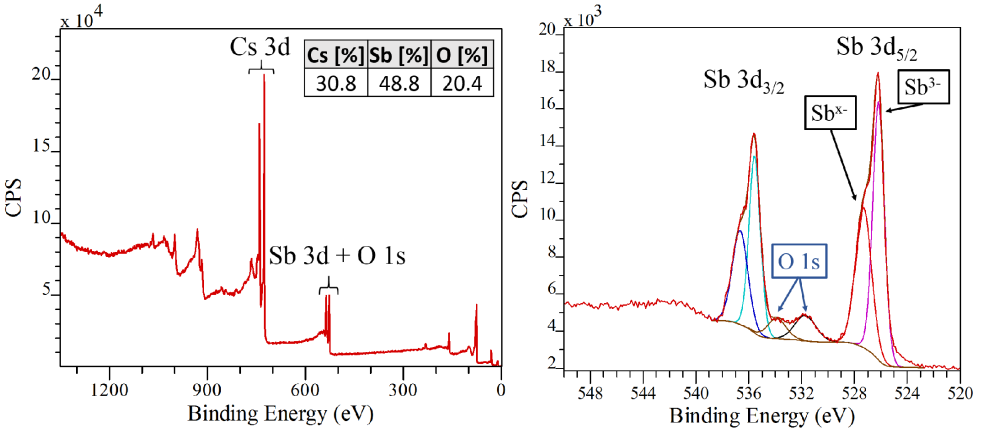

Fig.2. XPS measurements (Counts Per Second over Binding Energy) on cathode #202 (Cs_3Sb) as newly produced (a) wide range spectrum; (b) high resolution spectrum of Sb3d + O1s region (red line: measured spectrum, brown lines: Shirley background, other colours lines: fitting profiles, dark brown: overall fit-almost overlapping with the measured spectrum).

The cesium 3d levels (see Fig. 4 (b), red line) are shifted towards lower binding energy with respect to the free-metal (Cs $3d_{5/2}$=726.4 eV, Moulder et al. [15]) even if in the Cs-Sb compounds the alkali metal is transferring a large fraction of the electronic charge to the antimony. Such unusual behavior was already observed in previous XPS analysis of alkali antimonide surfaces and it can be explained by the predominantly ionic character of the Cs_3Sb structure (Bates et al. [11]). The satellite broad peaks at the left of the main photoemissive peaks, identified as plasmons, arise from the excitation of plasma oscillations of the valence band electrons by the motion of photoelectron in the solid. This pronounced feature was noticed to be associated with higher photosensitivity already by Bates et al. [11].

3.2. Measurements on cathode #202 (Cs_3Sb) after high average current lifetime measurements in the DC gun setup

The XPS analysis was performed again on the cathode #202 surface after lifetime measurements in the DC gun setup (Hessler et al. [6]). On the used cathode, both oxygen and carbon were detected, as shown by Fig. 3 (a).

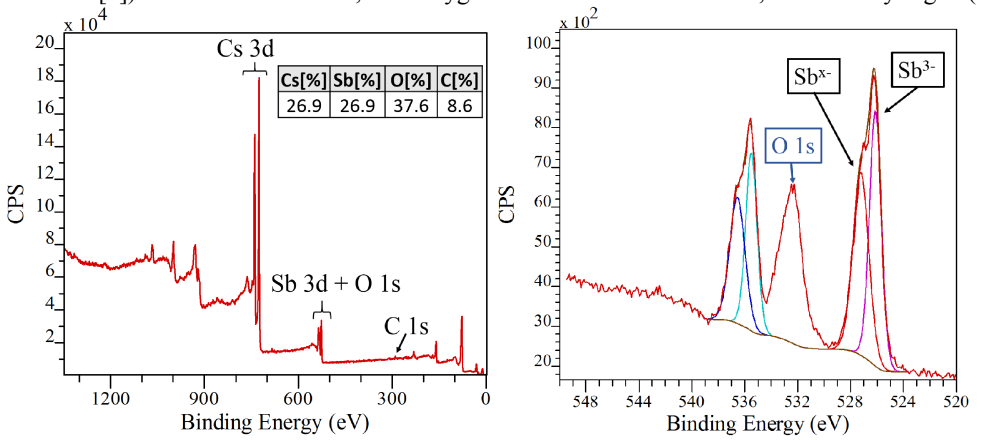

Fig.3. XPS measurements on used cathode #202 (Cs_3Sb) (a) wide range spectrum; (b) high resolution spectrum of Sb 3d + O 1s region with peaks model.

The relative elemental composition gives a Cs/Sb ratio close to 1, higher than the ratio measured on the new cathode surface. Nonetheless the cathode maximum QE decreased from 3.5% (Fig. 1 (a)) to 0.6% (Fig. 1 (b)).

The peaks model proposed in Fig. 3 (b) assumed that the same Sb compounds as found on the cathode surface as grown (Fig. 2 (b)) are still present on the cathode surface: the fitting peaks with the same position and the same width reproduce well the measured spectrum. The intensity of Sb 3d peaks as well as Cs 3d peaks (discussed later), instead, has decreased compared to the as grown cathode. This implies that the surface is covered with a contamination layer. Therefore a different depth of the photoemissive layer is probed through the XPS measurements for new and used cathode, which could explain the different Cs/Sb ratio.

The carbon contribution is clearly visible from the high resolution spectra of the C 1s region displayed in Fig. 4 (a), which is not the case on the as-grown cathode surface. Moreover a huge peak associated with oxygen is visible at 532.45 eV (FWHM=2 eV) in Fig. 3 (b). The degradation study of multialkali antimonide cathodes under controlled exposure of CO_2 performed by Michelato et al. [16], suggests that carbon dioxide could be effective also in degrading Cs_3Sb cathodes. Adsorbed CO_2 normally give rise to O 1s peak at higher binding energy (533.7-535.5 eV) as shown by XPS on different metals surface by Vishnu et al. [17]. Solymosi [18] reported instead the formation of carbonate on some metals after exposure to CO_2 at room temperature. Moreover, the position of the carbon peak (290.46 eV) is compatible with the C 1s level of the carbonate ion (CO_3^{2-}, as reported by Moulder [15]). Therefore it is likely that the cesium on the cathode surface has reacted with CO_2 forming cesium carbonates (Cs_2CO_3). It is not excluded that the broad oxygen peak labelled as O 1s in Fig. 3 (b) is the result of the coexistence of different chemical states of oxygen in addition to the cesium carbonate such as in Cs_3O_{11} or in H_2O, already found on the as-grown cathode surface.

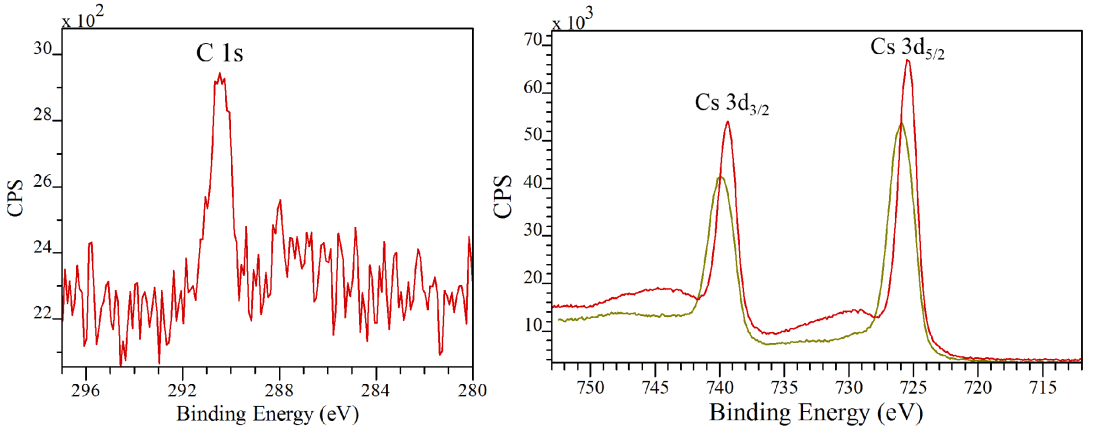

Fig.4. XPS high resolution spectra on cathode #202 (Cs_3Sb) (a) C 1s region on used cathode; (b) Cs 3d region on cathode surface as newly produced (red line) and as used (green line).

One more argument comes from the analysis of the high resolution XPS spectra of Cs 3d region displayed in Fig. 4 (b) with green line. These peaks are shifted towards higher binding energy compared to the measurements on the high quantum efficiency surface shown in red in the same plot. The higher peaks width (FWHM=2.2 eV compared to the 1.6 eV for the newly produced cathode) and the less pronounced plasmons structures are also indication of different composition due to the formation of different Cs chemical states on the cathode surface. The same tendency was observed by Bates et al. [11] on alkali antimonide photoemitters after the heating induced degradation of their photosensitivity. In this study the changes in the XPS high resolution spectra are specifically ascribed to the formation of the cesium carbonate.

3.3. Measurements on cathode #199 (Cs_3Sb) after beam tests in the PHIN RF photoinjector

Cathode #199 showed an average QE of 5.2% as newly produced (Fig. 5 (a)). After the measurements performed in the PHIN RF photoinjector (Hessler et al. [5]), its photoemissive properties were strongly deteriorated (Fig. 5 (b)).

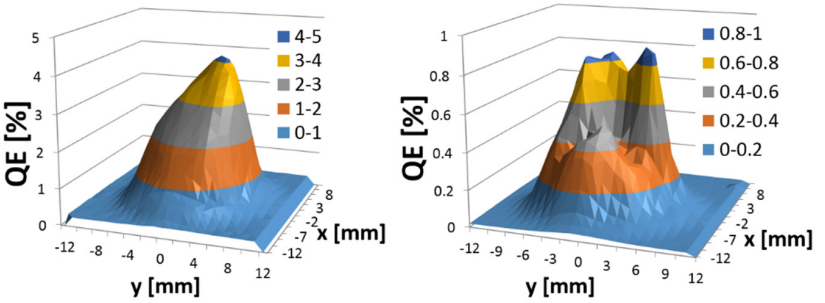

Fig. 5. QE maps of cathode #199 (Cs_3Sb) (a) as newly produced; (b) after beam tests in the PHIN RF photoinjector.

The wide range XPS spectrum shown in Fig. 6 (a) was taken on the surface of the used cathode.

Quantitative analysis of cathode #199 showed a strong deficiency of cesium compared to the desired compound Cs_3Sb. The Cs/Sb atomic ratio is 0.6 and the only contaminant that was found is oxygen.

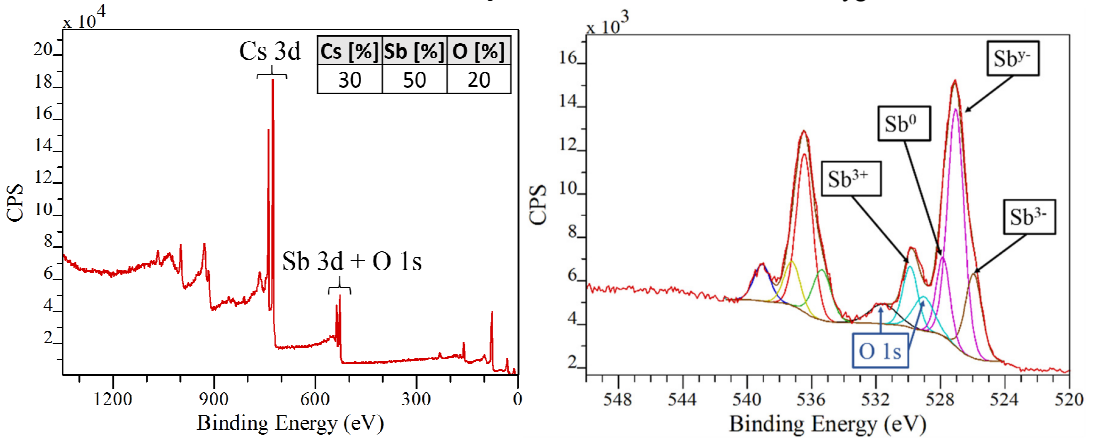

Fig. 6. XPS measurements on used cathode #199 (Cs_3Sb) (a) wide range spectrum; (b) Sb 3d and O1s region with peaks model.

The high resolution XPS spectrum in the region of antimony peaks with the result of an accurate fitting procedure is shown in Fig. 6 (b). This peaks model is interpreted as the occurrence on the cathode surface of four different chemical states of antimony. The most reasonable assignment of the peak at lower binding energy (525.9 eV) is to Sb^{3-} species as in the compound Cs_3Sb, in agreement with the analysis done on cathode #202. The other two antimony components are attributed to an alkali-deficient Cs-Sb compound (peak at 527 eV, as already explained in the previous sections) and to metallic antimony (Sb^0 at 527.9 eV, in good agreement with values recorded by Moulder [15]). Part of the antimony is bound as the oxide Sb_2O_3: well apart peak at 529.8 eV (labelled as Sb^{3+}). The same assignment was done by Soriano et al. [10] after oxidation of an alkali-deficient cesium antimonide. The residual oxygen O 1s contribution is split in two peaks: the peak at 531. 5 eV which is attributed to Cs_3O_{11} and a peak at about 529 eV which might be associated to the oxygen species in Sb_2O_3 (Martini et al. [19]). As explained by Soriano et al. [10] after even little oxygen exposure of K_2CsSb surface the cesium reacts with the oxygen to form Cs_3O_{11} and as a consequence,

elemental Sb (Sb^0) is segregated on the top layer. Similar behavior was reported by Bates et al. [11] while studying the effect of oxidation on alkali antimonide.

The good static vacuum level of the PHIN RF gun ($P=2x10^{-10}$ mbar) which is ensured by the upgraded vacuum system (Hessler et al. [12]) is nonetheless contaminated by induced O_2 desorption during beam production. It is likely therefore that the strong QE degradation is related to the oxidation (formation of Cs_3O_{11} and Sb_2O_3, Sb metal segregated at the surface) of the cathode surface during the photoinjector operation.

The origin of the big contribution of the alkali-deficient component is not fully understood. According to the presented analysis only 14% of the antimony content is in the form of Cs_3Sb, while the main contribution (27%) is attributed to an intermediate Cs-Sb phase with abundancy of antimony. The depletion of cesium could be due to high energy electrons/ions that might impinge on the cathodes surface. RF breakdowns are frequent during the gun operation and the ions back bombardment is a well-known cathode deteriorating effect (Poelker [20]). On the other hand, as discussed in Sec. 3.1, the Sb-rich phase could be produced during the deposition process if not enough cesium is available. The unavailability of XPS measurements on the same cathode surface before the tests in the RF photoinjector does not allow a conclusive explanation.

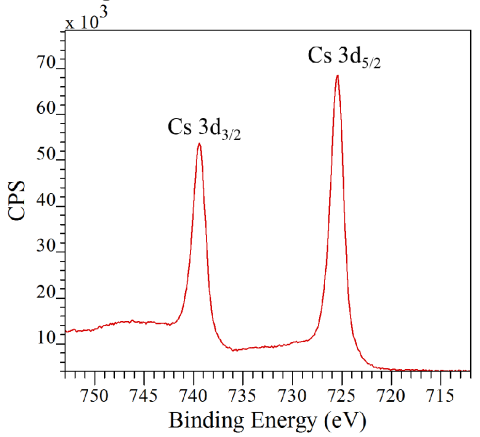

Fig. 7. XPS measurement on used cathode #199 (Cs_3Sb), high resolution spectrum of Cs 3d region.

Such a detailed study of the chemical states of cesium is limited by the small chemical shifts of the core levels between Cs metal, Cs-Sb compounds and Cs oxides (Bates et al. [11]). The XPS spectrum taken with high resolution in the Cs 3d region (Fig. 7) shows two sharp peaks (FWHM=1.6eV) and a weak plasmons structure only visible at the left of the Cs $3d_{3/2}$ peak. Such feature, which was discussed already in Sec. 3.2, is normally associated with low photosensitivity alkali antimonide surfaces.

4. Conclusion

The presented study shows that the cathodes production process is not optimized in terms of the final stoichiometry of the deposited layer. The variability of the QE values measured on newly produced cathodes could be explained as different level of alkali deficiency.

The QE degradation is explained in terms of the contamination of the cathode surface and formation of other Cs and Sb compounds. For the cathode #202, after measurements in the DC gun set up, no antimony oxides were detected. The QE deterioration is attributed to the adsorption of CO_2 and the subsequent formation of cesium carbonate. The coexistence of cesium sub-oxide and adsorbed water together with the carbonate is not excluded.

Cathode #199, measured after test in the RF photoinjector, shows a different surface composition: metal antimony and Sb_2O_3 were detected and no carbon was measured. The poor photoemissive properties of cathode#199-as used are

ascribed to such compounds as well as to Cs_3O_{11}. As pointed out in the introduction the environmental condition in the RF photoinjector are different with respect to the DC gun beam line, therefore different cathode detrimental processes (Poelker [20]) would be dominant in each setup. The pronounced non uniformity of the QE map of Fig. 5 (b) suggests that the impact of electrons/ions was involved in the degradation of the cathode surface. Carbon dioxide is also desorbed during the operation of the PHIN RF photoinjector, but the vacuum setup, equipped with Non Evaporable Getter (NEG) coating and NEG cartridge, has a higher capability of pumping it.

This analysis represents a step forward in the understanding of the different performance of the produced Cs_3Sb cathodes and their degradation processes. Final conclusion on the suitability of cesium antimonide cathodes for the specific application requires more studies, mainly related to the operation with beam parameters closer to the CLIC drive beam design parameters.

Acknowledgements

This project has received funding from the European Union's Seventh Framework Programme for research, technological development and demonstration under grant agreement no 289191. We acknowledge collaborators from the Laboratoire de l'Accélérateur Linéaire (LAL) for design and construction of the UHV transport carrier which enabled the XPS studies of the photocathodes.

References

[1] Geschonke G, Ghigo A. *CTF3 Note 2002-047*; 2002.
[2] Hessler C, Chevallay E, Divall Csatari M, Doebert S, Fedosseev V. Lifetime studies of Cs_2Te cathodes at the PHIN RF photoinjector at CERN. *Proc*. *IPAC 2012*; 2012.
[3] Chevallay E. Experimental Results at CERN Photoemission Laboratory with Co-deposition Photocathodes in the Frame of the CLIC Studies. *CTF3 Note 104*; 2012.
[4] Martini I, Chevallay E, Doebert S, Fedosseev V, Hessler C, Martyanov M. Studies of Cs_3Sb Cathodes for the CLIC Drive Beam Photoinjector Option. *Proc*. *IPAC 2013*; 2013.
[5] Hessler C, Chevallay E, Doebert S, Fedosseev V, Martini I, Martyanov M. Recent Results on the Performance of Cs_3Sb Photocathodes in the PHIN RF-gun. *Proc*. *IPAC 2015*; 2015.
[6] Hessler C, Chevallay E, Doebert S, Fedosseev V, Martini I, Martyanov M, publication in preparation.
[7] Spicer WE. Photoemissive, Photoconductive and Optical Absorption Studies of Alkali-Antomony Compounds. *Phis*. *Rev*.; 1958, Vol.112, p. 114.
[8] Sangster J, Pelton AD. The Cs-Sb (Cesium-Antimony) System. *Journal of Phase Equilibria 18*; 1997, Vol. 4, p. 382-386.
[9] Sommer AH. *Photoemissive materials*. John Wiley & Sons, Inc; 1968.
[10] Soriano L. Galan L. Interaction of Cesium-Potassium Antimonide Photocathode Materials with Oxygen: an X-ray Photoelectron Spectroscopy Study. *J*. *Appl*. *Phys*.; 1993, Vol 32, p. 4737-4744.
[11] Bates CW, van Atekum ThM Jr, Wertheim GK, Buchanan DNE, Clements KE. X-ray Photoemission Studies of Superficially Oxidized Cesium Antimonide Photoemitters. *Appl*. *Phys*. *Lett*.; 1981; Vol. 38, p.387-389.
[12] Hessler C, Chevallay E, Doebert S, Martini I, Perillo Marcone A, Sroka S. Recent Developments at the High-Charge PHIN Photoinjector and the CERN Photoemission Laboratory. *Proc*. *IPAC 2014*; 2014.
[13] Spitzer A, Luth H. An XPS Study of the Water Adsorption on Cu (100). *Surface Science*; 1985, Vol. 160, p. 353-361.
[14] Linn JH, Swartz WE Jr. An XPS Study of the Water Adsorption/Desorption Characteristics of Transition Metal Oxide Surfaces: Microelectronic Implications. *Applications of Surface Science*; 1984, Vol. 20, p.154-166.
[15] Moulder JF, Stickle WF, Sobol PE, Kenneth DB. *Handbook of X-ray Photoelectron Spectroscopy*. Perkin-Elmer Corporation, Physical Electronics Inc; 1993.
[16] Michelato P, Pagani C, Sertore D, Valeri S. Multialkali Thin Photocathodes for High Brightness guns. *Proc*. *EPAC1994*; 1994.
[17] Vishnu Kamath P., Rao CNR. Electron Spectrocopic Studies of Oxygen and Carbon Dioxide Adsorbed on Metal Surfaces. *J*. *Phys*. *Chem*. ; 1984, Vol. 88, p. 464-469
[18] Solymosi F. The Bonding, Structure and Reactions of CO_2 Adsorbed on Clean and Promoted Metal Surfaces, *Journal of Molecular Catalysis*; 1991, Vol. 65, p. 337-358.
[19] Martini I, Chevallay E, Fedosseev V, Hessler C, Neupert H, Nistor V, Taborelli M. Surface Characterization at CERN of Photocathodes for Photoinjector Applications. *Proc*. *IPAC 2015*; 2015.
[20] Poelker M. *USPAS Course on Photocathode Physics*; 2011, Lecture 8.